BIOCHEMISTRY

 Volume 46, Number 45 November 13, 2007

Accelerated Publications

Binding Energy in the One-Electron Reductive Cleavage of *S*-Adenosylmethionine in Lysine 2,3-Aminomutase, a Radical SAM Enzyme†

Susan C. Wang and Perry A. Frey*

Department of Biochemistry, University of Wisconsin—Madison, 1710 University Avenue, Madison, Wisconsin 53726

Received August 28, 2007; Revised Manuscript Received October 1, 2007

ABSTRACT: The common step in the actions of members of the radical SAM superfamily of enzymes is the one-electron reductive cleavage of *S*-adenosyl-L-methionine (SAM) into methionine and the 5′-deoxyadenosyl radical. The source of the electron is the $[4Fe\text{-}4S]^{1+}$ cluster characterizing the radical SAM superfamily, to which SAM is directly ligated through its methionyl carboxylate and amino groups. The energetics of the reductive cleavage of SAM is an outstanding question in the actions of radical SAM enzymes. The energetics is here reported for the action of lysine 2,3-aminomutase (LAM), which catalyzes the interconversion of L-lysine and L-β-lysine. From earlier work, the reduction potential of the $[4Fe\text{-}4S]^{2+/1+}$ cluster in LAM is −0.43 V with SAM bound to the cluster (Hinckley, G. T., and Frey, P. A. (2006) *Biochemistry 45*, 3219−3225), 1.4 V higher than the reported value for trialkylsulfonium ions in solution. The midpoint reduction potential upon binding L-lysine has been estimated to be −0.6 V from the values of midpoint potentials measured with SAM bound to the cluster and L-alanine in place of L-lysine, with *S*-adenosyl-L-homocysteine (SAH) bound to the cluster in the presence of L-lysine, and with SAH bound to the cluster in the presence of L-alanine or of L-alanine and ethylamine in place of L-lysine. The reduction potential for SAM has been estimated to be −0.99 V from the measured value for *S*-3′,4′-anhydroadenosyl-L-methionine. The reduction potential for the [4Fe-4S] cluster is lowered 0.17 V by the binding of lysine to LAM, and the binding of SAM to the [4Fe-4S] cluster in LAM elevates its reduction potential by 0.81 V. Thus, the binding of L-lysine to LAM contributes 4 kcal mol^{-1}, and the binding of SAM to the [4Fe-4S] cluster in LAM contributes 19 kcal mol^{-1} toward lowering the barrier for reductive cleavage of SAM from 32 kcal mol^{-1} in solution to 9 kcal mol^{-1} at the active site of LAM.

Members of the radical SAM[1] superfamily catalyze a diverse array of biochemical processes through mechanisms with free radical intermediates (*1*−*10*). Radical SAM enzymes participate in amino acid metabolism; biosynthesis of coenzymes such as biotin, lipoic acid, thiamine pyrophosphate, molybdopterin, heme in anaerobic bacteria, and pyrroloquinoline quinone among others; DNA biosynthesis

† This research was supported by NIH Grant DK28607 from the National Institute of Diabetes and Digestive and Kidney Diseases.

* To whom correspondence should be addressed. Department of Biochemistry, University of Wisconsin—Madison, 1710 University Ave., Madison, WI 53726. Tel: (608) 262-0055. Fax: (608) 265-2904. E-mail: frey@biochem.wisc.edu.

[1] Abbreviations: Ado•, the 5′-deoxyadenosyl radical; *an*Ado•, the 3′,4′-anhydro-5′-deoxyadenosyl radical; *an*ATP, 3′,4′-anhydroadenosine triphosphate; *an*SAM, *S*-3′,4′-anhydroadenosyl-L-methionine; EDTA, ethylenediaminetetraacetic acid; EPPS, 4-(2-hydroxyethyl)-1-piperazinepropanesulfonic acid; G, Gauss; EPR, electron paramagnetic resonance; HPLC, high performance liquid chromatography; LAM, lysine 2,3-aminomutase; Met, methionine; PLP, pyridoxal-5′-phosphate; SAH, *S*-adenosyl-L-homocysteine; SAM, *S*-adenosyl-L-methionine; SeSAM, Se-adenosyl-L-selenomethionine.

10.1021/bi701745h CCC: $37.00
Published on Web 10/18/2007

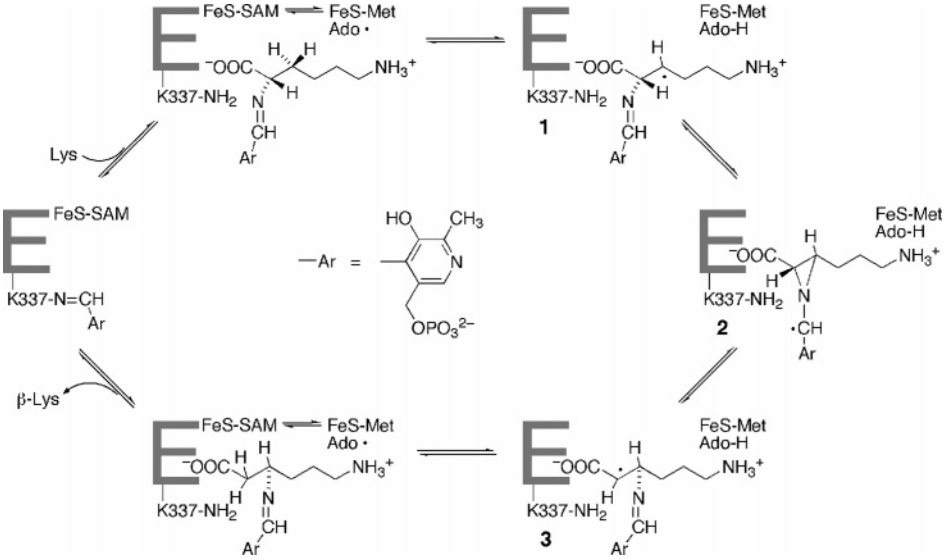

FIGURE 1: The currently accepted mechanism of action of LAM. Kinetic and EPR spectroscopic evidence for the radical complexes **1** and **3** and the radical Ado• as intermediates has been published (*3*, *5*, *19*). The present work relates to the energetics for the reductive cleavage of SAM ligated to the FeS-cluster.

and repair; and the biosynthesis of a variety of antibiotics. The radical SAM enzymes incorporate specialized iron−sulfur clusters nucleated by the cysteine motif CxxxCxxC, and the three cysteine-residues within this motif account for three ligands to iron in the [4Fe-4S] centers. The fourth ligand is SAM itself, with the methionyl amino and carboxylate groups serving as a bidentate ligand to the non-cysteine-ligated iron of the cluster (*11*−*13*).

Very few of the reaction mechanisms in the radical SAM superfamily are known in detail. Available information indicates that radical SAM enzymes share one process in common, the one-electron reductive cleavage of SAM to the 5-deoxyadenosyl radical and methionine (*1*−*10*). The electron for reductive cleavage arises from the $[4Fe\text{-}4S]^{1+}$ cluster, according to eq 1,

$$E\text{-}[4Fe\text{–}4S]^{1+}\text{-SAM} \rightleftharpoons E\text{-}[4Fe\text{–}4S]^{2+}\text{-Met.Ado}\bullet \quad (1)$$

where Ado• represents the 5′-deoxyadenosyl radical and Met is methionine. Ado• initiates catalysis by abstracting a hydrogen atom from a substrate to generate 5′-deoxyadenosine and a substrate-related radical as initial intermediates. Subsequent steps in the mechanisms of the overall reactions are as diverse as the reactions themselves. The most thoroughly documented radical mechanism among members of this family is that of lysine 2,3-aminomutase (LAM) shown in Figure 1 (*3*, *5*). Three of the four radical intermediates have been identified and characterized spectroscopically and kinetically.

A general mechanistic problem in the radical SAM superfamily is the one-electron reductive cleavage of SAM. The reduction potentials (2+/1+) of the [4Fe-4S] clusters in the family are far less negative than the reported values for the irreversible one-electron reduction of trialkylsulfonium ions such as SAM, which are approximately −1.8 V (*14*−*16*). In the case of LAM, the (2+/1+)-reduction potential of the [4Fe-4S] cluster with SAM ligated to the cluster is −430 mV (*17*), so that the barrier to the one-electron reductive cleavage of SAM should be about −1.4 V, corresponding to 32 kcal mol^{-1}. The barrier must be much lower in the active site of LAM; otherwise the rate constant for the slowest step in the mechanism would have to be about 4×10^{22} s^{-1}, many orders of magnitude larger than typical bond vibrational frequencies.[2] We report the effect of binding lysine to the active site on the reduction potential (2+/1+) of the [4Fe-4S] cluster, we measure the equilibrium constant for reductive cleavage of *S*-3′,4′-anhydroadenosyl-L-methionine (*an*SAM) at the active site in the presence of lysine, we calculate the corresponding equilibrium constant for SAM, and we estimate the energetic contributions of binding lysine and SAM to decreasing the energy barrier to reductive cleavage of SAM.

EXPERIMENTAL PROCEDURES

Materials. 4,4′-Dimethyl-1,1′-trimethylene-2,2′-dipyridyl bromide and 1,1′-trimethylene-2,2′-dipyridyl bromide were synthesized as described (*18*). *an*ATP was synthesized previously (*19*) and stored at −70 °C until use. *an*SAM was used either as a stock solution frozen at −70 °C or synthesized and frozen at −70 °C without further purification. Other reagents were purchased from Thermo Fisher Scientific (Waltham, MA), MP Biomedicals (Irvine, CA), or Sigma-Aldrich (St. Louis, MO) unless otherwise indicated. SAM synthetase was purified as described (*20*, *21*). 4,4′-Dimethyl-1,1′-tetramethylene-2,2′-dipyridyl bromide was synthesized according to previously reported methods (*18*, *22*) with the following modifications: Stoichiometric amounts

[2] If the one-electron reductive cleavage of SAM at the active site is fast and at equilibrium during catalysis, the estimated $\Delta E°$ of −1.4 V in solution means that the equilibrium constant for the formation of Ado• from SAM at the active site should be 10^{-23} if the reduction potential of SAM at the active site is the same as in solution. The turnover number for LAM is about 40 s^{-1} under initial rate conditions, that is, in the absence of the product. Then at saturating lysine, 1 μM LAM will generate β-lysine at the rate of 40 μM s^{-1}, and this rate must be attained with the Ado•-containing intermediate at a concentration of about 10^{-23} μM, given the postulated equilibrium constant for its formation. If this were the case, the rate constant for the reaction of Ado• in the irreversible formation of the product would be 40 μM $s^{-1}/10^{-23}$ μM, or 4×10^{22} s^{-1}, an unreasonable value. Thus, the equilibrium constant for the formation of Ado• cannot be 10^{-23} and the value of $\Delta E°$ at the active site cannot be the solution value of −1.4 V.

of the starting materials, 4,4′-dimethyl-2,2′-dipyridyl (0.5 g) and 1,4-dibromopropane (300 μL) were mixed and heated in anisole (28 mL) at reflux for ~24 h under Ar in the dark. The resulting solid was filtered and washed with acetone. The dried product was dissolved in methanol (0.5 mL) and recrystallized using acetone (~10 mL).

Enzyme Production, Purification, Reconstitution, and Characterization. Recombinant LAM was purified and reconstituted as described (*17*, *23*, *24*). Reconstitution of iron−sulfur clusters was performed for 12−15 h at room temperature in an anaerobic chamber (Coy Laboratory Products, Grass Lake, MI). Amicon Ultra-15 Centrifugal Filter Units (30,000 MWCO) from Millipore (Billerica, MA) placed in sealing 250 mL centrifuge bottles were used to concentrate the protein. Iron and sulfide analyses were performed as described (*25*, *26*). Protein concentrations were determined by comparing the absorbance at 280 nm with the extinction coefficient for reconstituted LAM as determined by amino acid analysis ($\epsilon = 7.63 \times 10^4$ subunit M^{-1} cm^{-1}; *27*). LAM was assayed for activity as described (*28*) with minor modifications.

Anhydroadenosyl Radical Formation. Due to the instability of *an*SAM, the cofactor analogue was prepared *in vitro* and stored at −70 °C without further purification. The reaction was performed in the anaerobic chamber and monitored by HPLC. Each reaction contained 50 mM EPPS (pH 8.0); 20 mM $MgSO_4$; 3.25 mM *an*ATP; 3.52 mM methionine; 40 μg of inorganic phosphatase (Sigma-Aldrich, St. Louis, MO); and sufficient SAM synthetase to ensure that the reaction had gone to completion after 30 min. The reaction was fast-frozen in liquid nitrogen prior to storage.

Prior to use, frozen *an*SAM was thawed in the anaerobic chamber and vacuum purged and flushed with argon (15+ cycles) to remove oxygen. A mix was prepared containing all components except LAM. Aliquots (230 μL) of the mix were allocated, and addition of the enzyme (20 μL) initiated the reaction. The resulting mixture was rapidly transferred into an EPR tube and frozen in cold isopentane (~ −50 °C) at time points ranging from 15 to 75 s. Duplicates were created for each time point, and the average radical concentration is illustrated in Figure 2. Final concentrations of the reaction components were 34 μM (subunit) LAM; 200 mM EPPS, pH 8.0; 320 μM sodium dithionite; 510 μM *an*SAM; 16 mM lysine (free base). For comparison, samples were set up with no lysine and *an*SAM or with SAM (tosylate salt, 400 μM) and 4-thia-L-lysine (*S*-2-aminoethyl-L-cysteine hydrochloride, 10 mM). The final concentration of sodium dithionite, which was significantly lower than previously employed (*19*), was determined by titrating dithionite (100 μM to 1 mM) against the protein while observing the +1 signal from the iron−sulfur cluster by EPR. It was important to optimize the dithionite concentration because excess dithionite could lead to over-reduction of $[4Fe\text{-}4S]^{2+}$ on the right side of eq 1, with consequent overproduction of *an*Ado• from *an*SAM. Controls were performed using SAM generated *in vitro* with SAM synthetase showing that the presence of the additional enzyme and associated components (i.e., Mg^{2+}, methionine, and phosphate) did not interfere with signal intensity.

Spectroelectrochemistry. Spectroelectrochemical titrations were performed as described elsewhere (*17*) with minor modifications. After reducing the sample for 15 min at a controlled potential, which was monitored for 75 s to track the drift that occurs during sample transfer. The sample was reduced again for 5 min, transferred into the EPR tube, and the transfer time recorded. The corresponding potential from the time course of drift was used for data analysis. A typical mixture contained ~1 mg of reconstituted LAM, 150 mM EPPS (pH 8.0), 67 mM K_2SO_4 (as an electrolyte), 100 μM each of 4,4′-dimethyl-1,1′-trimethylene-2,2′-dipyridyl bromide and 1,1′-trimethylene-2,2′-dipyridyl bromide or 4,4′-dimethyl-1,1′-tetramethylene-2,2′-dipyridyl bromide, and 425 μM of the appropriate adenosyl cofactor or analogue. Final substrate and substrate analogue concentrations, when present, were as follows: 100 mM alanine, 100 mM ethylamine, 40 mM lysine.

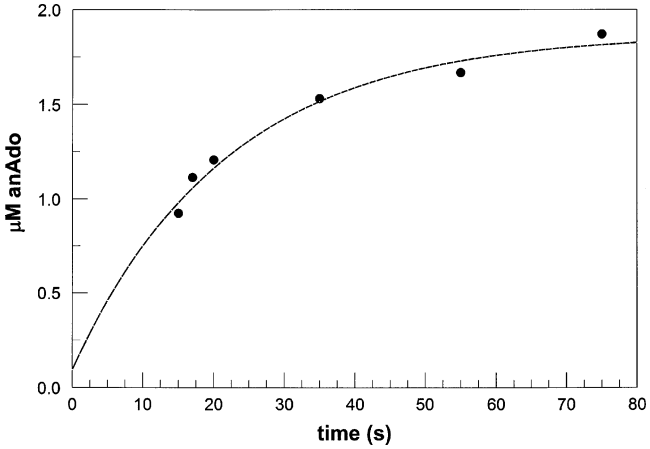

FIGURE 2: Equilibrium in the reductive cleavage of *an*SAM at the active site of LAM. *an*SAM in place of SAM at the active site of LAM is reductively cleaved to the radical *an*Ado• upon reaction with lysine (*19*). The figure shows the increase with time of the EPR signal for *an*Ado• after addition of lysine to 34 μM LAM. The reaction proceeds to equilibrium at 2 μM *an*Ado•. Although lysine is a poor substrate and reacts forward very slowly, the cleavage of *an*SAM to the radical *an*Ado• approaches equilibrium. The detailed composition of the reaction mixture is given in Experimental Procedures.

EPR Spectroscopy and Data Analysis. Low-temperature X-band EPR spectra were acquired on a Varian Line spectrometer equipped with a Varian E102 microwave bridge and interfaced with a Linux system. Spectra were obtained and manipulated using the Xemr program (Jussi Eloranta, http://www.csun.edu/~jeloranta/xemr). An Oxford Instruments ESR-900 continuous flow helium flow cryostat and Oxford Instruments 3120 temperature controller were used. A Varian gaussmeter and a Hewlett-Packard 5255A frequency converter and 5245L electronic counter were employed to measure the magnetic field strength and the frequency, respectively. A Hewlett-Packard 432A power meter was used to calibrate the microwave power. Spectra were acquired as the average of four 2 min scans. Conditions for iron−sulfur EPR were as follows: 9.252 GHz, 16 G modulation amplitude, 3400 G center field, 1000 G sweep width, 1−5 mW power, 1600−8000 gain, 0.3 s time constant, 10 K. Conditions for radical EPR were 9.252 GHz, 4 G modulation amplitude, 3300 G center field, 400 G sweep width, 15 μW power, 2000 gain, 0.3 s time constant, 10 K. Spin concentrations were estimated by double integration of spectra using a copper standard (1 mM $CuSO_4$, 10 mM EDTA) at 15 μW and 10 K as a reference. Data analysis

Table 1: Reduction Potentials for $[4Fe\text{-}4S]^{2+/1+}$ in Selected Complexes of LAM

complex	$E°$ (m*V*)[a]	ref
E-[4Fe-4S]-SAM.PLP	−430 ± 2	*17*
E-[4Fe-4S]-SAH.PLP	−460 ± 3	*17*
E-[4Fe-4S]-*aza*SAM.PLP	−497 ± 10	*17*
E-[4Fe-4S]-*an*SAM.PLP	−484 ± 5	this work
E-[4Fe-4S]-SAM.PLP=Ala	−582 ± 6	this work
E-[4Fe-4S]-SAH.PLP=Ala	−566 ± 6	this work
E-[4Fe-4S]-SAH.PLP=Ala/ $EtNH_3^+$	−594 ± 17	this work
E-[4Fe-4S]-SAH.PLP=Lys	−583 ± 21	this work

[a] All midpoint potentials are measured at pH 8.0 and are pH-independent.

was performed as described elsewhere (*17*) using the program PSI-Plot (Poly Software International, Pearl River, NY).

RESULTS

Midpoint Reduction Potential of [4Fe-4S] Bound to LAM in the Michaelis Complex. The one-electron midpoint reduction potential of the $[4Fe\text{-}4S]^{2+/1+}$ center with SAM bound to the active site as a ligand to the cluster is −430 mV (*17*). This value ensures that the iron−sulfur cluster can be reduced to the (1+) state *in vivo* by biological systems (*29*). All reduction potentials and equilibrium constants in this paper refer to pH 8.0; reduction potentials for sulfonium ions are pH-independent (*15*).

The potential of −430 mV is not necessarily relevant to the reductive cleavage of SAM in the active site because of the absence of the substrate lysine under the conditions of measurement. The most relevant reduction potential for the iron−sulfur cluster would be that of the Michaelis complex, which contains lysine and SAM and is poised for reaction. Measurement of that value would be impractical because with lysine present the reaction would proceed.

An estimate of the midpoint reduction potential for the iron−sulfur cluster in the Michaelis complex, which may be represented as **E**-$[4Fe\text{-}4S]^{1+}$-SAM. Lys, may be obtained from the midpoint potentials for complexes that are not reactive but are structurally similar to the Michaelis complex. Such complexes have SAH in place of SAM, or alanine in place of lysine, or alanine and ethylamine in place of lysine. Alanine is practically unreactive with LAM but is rescued as a substrate by the presence of ethylamine.[3] Values of midpoint potentials for such complexes are presented in Table 1. The results show that the binding of lysine or alanine significantly lowers the midpoint potentials. The binding of alanine to LAM with SAM lowers the potential by about 150 mV, and with SAH in place of SAM alanine lowers the potential by about 106 mV. Alanine should not be as effective as lysine, and this expectation is supported by the fact that lysine lowers the midpoint potential of the complex with SAH by 17 mV more than alanine. Furthermore, the addition of both alanine and ethylamine to the complex with SAH lowers the potential by 28 mV more than the addition of alanine alone.

It appears that the lysyl side chain induces a 17 to 28 mV lowering of the midpoint potential. When employed to adjust the midpoint potential of −582 mV measured for the complex with SAM and alanine, we can expect the value for SAM and lysine to lie between −599 and −610 mV. For the present purpose, shall adopt the value −600 mV as a conservative estimate of the midpoint potential for [4Fe-4S] in the Michaelis complex.

The Midpoint Potential for Reductive Cleavage of SAM in the Active Site. We wish to estimate the midpoint reduction potential for one-electron reductive cleavage of SAM at the active site of LAM ($E°_2$) according to eq 3. A value can be calculated if we have $\Delta E°$ for the overall reaction of eq 4, because we know $E°_1$ for the half-reaction in eq 2 from the foregoing section. A value for the equilibrium constant in the reaction of eq 4 is needed to calculate $\Delta G°_{pH8}$ from the relation $\Delta G°_{pH8} = -RT \ln K_{eq}$, and $\Delta E°$ can then be calculated from $\Delta G°_{pH8} = -nF\Delta E°$,

E-$[4Fe\text{–}4S]^{1+}$-SAM. Lys ⇌ **E**-$[4Fe\text{–}4S]^{2+}$-SAM. Lys + e^- $E°_1 = +600$ mV (2)

E-$[4Fe\text{–}4S]^{2+}$-SAM. Lys + e^- ⇌ **E**-$[4Fe\text{–}4S]^{2+}$-Met.Ado•. Lys + e^- $E°_2$ (3)

E-$[4Fe\text{–}4S]^{1+}$-SAM. Lys ⇌ **E**-$[4Fe\text{–}4S]^{2+}$-Met.Ado•. Lys $\Delta E° = E°_1 + E°_2$ (4)

where $n = 1$ electron and $F =$ Faraday constant (23 kcal mol^{-1} V^{-1}). The equilibrium constant for reaction 4 cannot be measured directly because the product reacts forward too rapidly, and in any case the value is too small to be measured by available analytical methods. The value can be estimated from the equilibrium constant for the related reaction 5 and the relative enthalpies of the 5′-deoxyadenosyl radical (Ado•) and the 3′,4′-anhydro-5′-deoxyadenosyl radical (*an*Ado•).

E-$[4Fe\text{–}4S]^{1+}$-*an*SAM.Lys ⇌ **E**-$[4Fe\text{–}4S]^{2+}$-Met.*an*Ado•.Lys (5)

The radical *an*Ado• is the EPR spectroscopically observed analogue of Ado• that appears when LAM is activated by *an*SAM, the corresponding analogue of SAM (*19*, *30*). The results in Figure 2 allow the value of K_{eq} for eq 5 in the reaction of *an*SAM to be calculated as 6.2×10^{-2}, which corresponds to $\Delta G°_{pH8} = 1.6$ kcal mol^{-1} for reaction 5. The calculation of 0.062 for the equilibrium constant is based on the subunit concentration of LAM and the assumption that the subunits function independently. LAM is a dimer of intercalated dimeric units, and if it should happen that only one subunit of the intimate dimer is functional, that is if the enzyme functions in a half-of-the-sites mode, then the equilibrium constant would be 0.12. This difference or uncertainty of a factor of 2 in the equilibrium constant would have a minor effect on the overall energetics in the reductive cleavage of SAM (∼2 kcal mol^{-1}).

We have confidence that the plateau in Figure 2 signals equilibrium in eq 5, the formation of *an*Ado•, because of the available information about this radical (*19*). *an*SAM functions normally as a coenzyme in place of SAM, albeit at a much slower rate. The slow rate is due to the stability of *an*Ado•, which is an allylic radical and much less reactive than Ado• in abstracting the hydrogen atom from the 3-pro-*R* position of the lysyl side chain. The value of the deuterium kinetic isotope effect in the reaction of deutero-lysine shows that hydrogen abstraction by *an*Ado• limits the rate. The slow overall rate, the large deuterium kinetic isotope effect, and the observation of *a*nAdo• as the sole free radical in the reaction all indicate equilibrium at the first hydrogen transfer step, the process in eq 5.

[3] F. J. Ruzicka and P. A. Frey, manuscript in preparation.

A value of $\Delta G°_{pH8}$ for eq 4 can be calculated from $\Delta G°_{pH8}$ for eq 5 and the relative energies of Ado• and *an*Ado•. From the Co−C5′ bond dissociation energy of 31 kcal mol^{-1} for adenosylcobalamin (*31*) and the bond dissociation energy of 24 kcal mol^{-1} for 3′,4′-anhydroadenosylcobalamin (*32*) the enthalpy difference between Ado• and *an*Ado• is 7 kcal mol^{-1}. If the entropy changes in the reactions of eqs 4 and 5 are the same or very similar, the enthalpy difference will be very near the free energy difference for these radicals at the active site of LAM. Inasmuch as both reactions occur within the confines of the active site, which contains no water or other molecules that might be dissociable (*33*), the assumption of similar or identical entropy changes in the two reactions seems reasonable. On that basis, a value of $\Delta G°_{pH8}$ for reaction 4 can be estimated by correcting the standard free energy of reaction 5 for the energy difference between the two radicals. An estimate of $\Delta G°_{pH8}$ for reaction 4 is then 8.6 kcal mol^{-1}, and the value of $\Delta E°$ is −390 mV. From the values $\Delta E° = -390$ mV for eq 4 and $E°_1 = +600$ mV for eq 2, the midpoint potential for reductive cleavage of SAM in eq 3 can be calculated as $E°_2 = -990$ mV.

*The Substrate-Related Radical in Reaction of 4-Thia-*L*-lysine.* LAM activated by SAM catalyzes the transformation of 4-thia-L-lysine into ethylamine and formylacetate (malonate semialdehyde). The cleavage products arise from the chemical decomposition of the enzymatic product, 4-thia-β-lysine, generated by the action of LAM on 4-thia-L-lysine as a substrate (*28*, *34*). In the steady state of the reaction of 4-thia-L-lysine, the only observable free radical is the 4-thialysyl-3-yl species, the 4-thia-analogue of the substrate-related radical **1** Figure 1, with the unpaired electron formally on C3 of the lysyl side chain. LAM activated by *an*SAM also accepts 4-thia-L-lysine as a substrate, and in the steady state a mixture of the substrate-related radical and *an*Ado• are observed by EPR spectroscopy, indicating that the two radicals are of comparable stability (*19*). The measured concentration of the 4-thia-analogue of radical **1** in Figure 1 in the reaction of 34 μM LAM activated by SAM is 2.9 μM, which corresponds to $K_{eq} = 0.087$ in the formation of the 4-thialysine-3-yl radical. Comparison of this value with 0.062 for the generation of anAdo• confirms the relative stabilities of the 4-thialysyl-3-yl and *an*Ado• radicals at the active site of LAM.

DISCUSSION

The one-electron reductive cleavage of trialkylsulfonium ions leads to alkyl radical products. Both electrolytic reduction at electrodes and chemical reduction by low potential iron sulfur clusters of the type [4Fe-4S(SR)$_4$] in acetonitrile effect electron transfer-induced cleavages to radicals (*14*, *16*, *35*). The chemical cleavages by [4Fe-4S-(SR)$_4$] in acetonitrile appear similar to the processes in radical SAM enzymes, but they are mechanistically unlike the enzymatic reactions. The chemical reactions of [4Fe-4S(SR)$_4$] involve very low potential clusters ($E° = -1.2$ V in acetonitrile) and highly reactive sulfonium ions ($E° = -0.9$ V). Reductive cleavages can take place through energetically downhill electron transfer in the absence of a kinetic barrier (*35*). The enzymatic reactions occur with [4Fe-4S]$^{2+/1+}$ transitions displaying $E° = -0.4$ to -0.5 V (*17*, *36*, *37*); they involve SAM as the trialkylsulfonium ion, with $E° \sim -1.8$ V as discussed in a following section; and SAM is ligated to the cluster, allowing inner sphere electron transfer (*11*−*13*, *32*, *37*−*41*).

The present results allow us to describe how binding energy is employed to decrease the energy barrier in the one-electron reductive cleavage of SAM at the active site of LAM. The barrier arises because of the difference between the one-electron reduction potential of the [4Fe-4S]$^{2+/1+}$ cluster with SAM ligated to the unique iron (−430 mV) and the one-electron irreversible reduction potentials for trialkylsulfonium ions in solution, which can be estimated to be −1800 mV. The potential −1800 mV may accepted as reasonable based on the reported value of −1850 mV for trimethylsulfonium and values of −1600 to −1650 mV for methyl alkyl aryl sulfonium ions (*14*−*16*). Aryl substituents elevate the potentials due to inductive electronic effects, and higher alkyl groups lead to less unstable radicals than methyl groups. The sulfonium group in SAM does not include an aryl substituent but does include two higher alkyl substituents, so the reduction potential will be slightly less negative than that of trimethylsulfonium ion (−1850 mV) but lower than if there were an aryl, vinyl, or allyl substituent. The value may lie between −1750 and −1800 mV, and we adopt −1800 as a rounded value in two significant figures.

The foregoing considerations lead to the free energy levels illustrated in Figure 3. The reduction potential of the iron−sulfur cluster in the resting enzyme, with cysteine as the ligand to the unique iron in the cluster, is −484 mV (*17*). When SAM binds to the cluster, the potential is elevated to −430 mV (Table 1), making reduction of the cluster to the 1+-state readily accessible to biological reducing systems (*29*). Upon binding lysine, the potential is lowered to −600 mV, still 1.2 V more positive than that of a free trialkylsulfonium ion. The reduction potential of free SAM may be estimated as that for one-electron irreversible reduction of a trialkylsulfonium ion, −1800 mV. However, when ligated to the [4Fe-4S] cluster in the active site of LAM, the calculated value is −990 mV, 810 mV higher. The difference between midpoint potentials for SAM and the [4Fe-4S] cluster in the active site of LAM is 390 mV, 1400 mV less than it would be in solution. While the values of $E°$ and $\Delta G°_{pH8}$ in this paper refer to pH 8.0, they are pH-independent and should be the same at pH 7.0.

Figure 3 shows that the binding of both lysine and SAM to LAM contributes to decreasing the barrier to the reductive cleavage of SAM. Lysine binding contributes 170 mV or 4 kcal mol^{-1}, and the binding of SAM to the [4Fe-4S]$^{1+}$ cluster contributes 810 mV or 19 kcal mol^{-1} to decreasing the barrier from 32 to 9 kcal mol^{-1}.

The elevated reduction potential of SAM in the active site of LAM can be attributed largely to its ligation to the [4Fe-4S] cluster. Ligation to Fe$^{2.5+}$ can by itself be expected to elevate the potential to some degree, even though the locus of ligation through the methionyl amino and carboxyl groups appears chemically remote from the sulfonium center. A further consideration in this phenomenon is the mechanism of electron transfer, shown in Scheme 1 (*11*, *33*, *38*). In the mechanism, electron transfer is accompanied by the transformation of pentacoordinate iron in [4Fe-4S]$^{1+}$ into hexacoordinate iron in [4Fe-4S]$^{2+}$, a more favored coordination state for iron. The coordination transition can be expected to contribute to easing electron transfer to the sulfonium group. Not least important is the fact that the mechanism

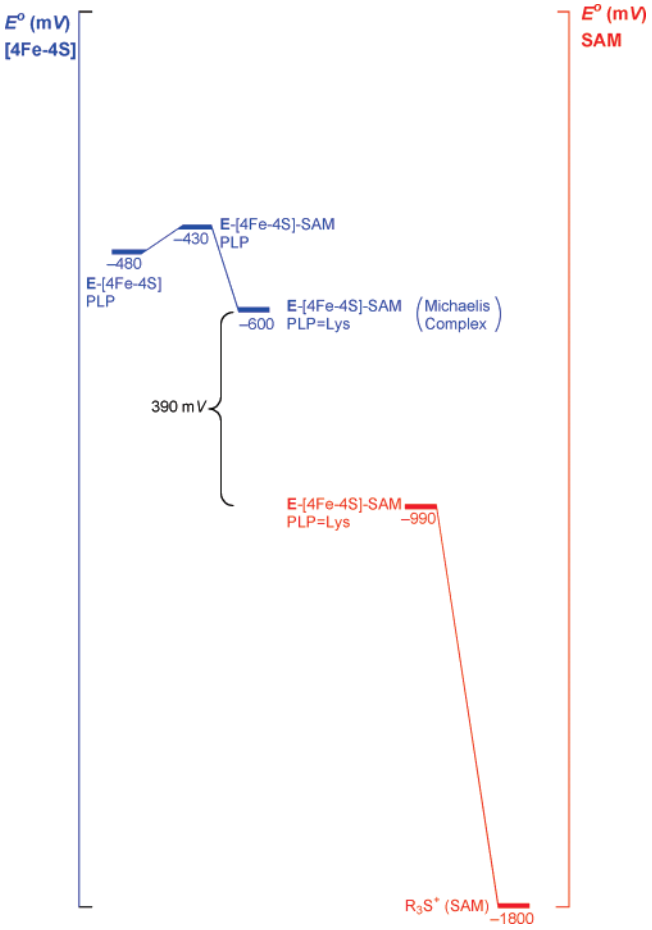

FIGURE 3: Energetics of one-electron reversible cleavage of SAM at the active site of LAM. The blue scale on the left illustrates the midpoint reduction potentials of the $[4Fe\text{-}4S]^{2+/1+}$ cluster with cysteine as the ligand, with SAM as the ligand, and with lysine bound and SAM as the ligand. The red scale shows the potentials for irreversible one-electron reduction of trialkylsulfonium ions, such as SAM, in solution and for reversible one-electron reductive cleavage of SAM bound to the [4Fe-4S] cluster in the active site of LAM.

Scheme 1

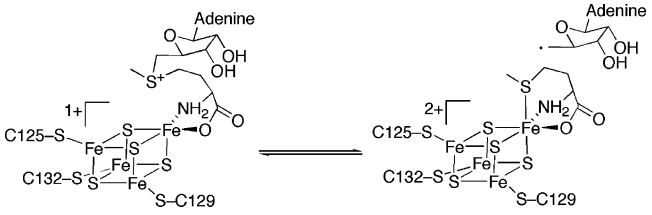

facilitates inner-sphere electron transfer. The structure shows Se in SeSAM within van der Waals distance of Fe in the cluster (*33*) so that the electron is transferred in the process of bond formation between Fe and Se, or Fe and S in the case of SAM, and does not have to traverse a significant distance through a medium.

The present work also measures the effect of the binding of lysine to lowering the reduction potential of the [4Fe-4S] center without explaining the molecular basis. The structure shows lysine bound as the external aldimine to PLP in very close proximity to the complex of SAM and the [4Fe-4S]. The presence of lysine in the site can be expected to limit exposure of the iron−sulfur cluster to the solvent. The question of whether this brings about a lowering of the reduction potential remains for future research.

ACKNOWLEDGMENT

We thank Glen T. Hinckley for insightful discussions and synthesizing 4,4′-dimethyl-1,1′-trimethylene-2,2′-dipyridyl bromide and 1,1′-trimethylene-2,2′-dipyridyl bromide; Frank Ruzicka for supplying LAM and for experimental assistance; Olafur Magnusson for a sample of *an*SAM and for supplying *an*ATP; Dawei Chen for supplying SAM synthetase; Russell Poyner and George Reed for assistance with the operation of the EPR spectrometer.

REFERENCES

1. Sofia, H. J., Chen, G., Hetzler, B. G., Reyes-Spindola, J. F., and Miller, N. E. (2001) Radical SAM, a novel protein superfamily linking unresolved steps in familiar biosynthetic pathways with radical mechanisms: functional characterization using new analysis and information visualization methods, *Nucleic Acids Res. 29*, 1097−1106.
2. Cheek, J., and Broderick, J. B. (2001) Adenosylmethionine-dependent iron-sulfur enzymes: versatile clusters in a radical new role, *J. Biol. Inorg. Chem. 6*, 209−226.
3. Frey, P. A., and Booker, S. J. (2001) Radical mechanisms of *S*-adenosylmethionine-dependent enzymes, *Adv. Protein Chem. 58*, 1−45.
4. Fontecave, M., Mulliez, E., and Ollagnier-de-Choudens, S. (2001) Adenosylmethionine as a source of 5′-deoxyadenosyl radicals, *Curr. Opin. Chem. Biol. 5*, 506−511.
5. Frey, P. A., and Magnusson, O. Th. (2003) *S*-Adenosylmethionine: A wolf in sheep's clothing or a rich man's adenosylcobalamin?, *Chem. Rev. 103*, 2129−2148.
6. Marsh, E. N., Patwardhan, A., and Huhta, M. S. (2004) *S*-Adenosylmethionine radical enzymes. *Bioorg. Chem. 32*, 326−440.
7. Jarrett, J. T. (2003) The generation of 5′-deoxyadenosyl radicals by adenosylmethionine-dependent radical enzymes, *Curr. Opin. Chem. Biol. 7*, 174−182.
8. Jarrett, J. T. (2005) The novel structure and chemistry of iron-sulfur clusters in the adenosylmethionine-dependent radical enzyme biotin synthase, *Arch. Biochem. Biophys. 433*, 312−321.
9. Layer, G., Kervio, E., Morlock, G., Heinz, D. W., Jahn, D., Rétey, J., and Schubert, W. D. (2005) Structural and functional comparison of HemN to other radical SAM enzymes, *Biol. Chem. 386*, 971−980.
10. Wang, S., and Frey, P. A. (2007) *S*-Adenosylmethionine as an oxidant: The radical SAM superfamily. *Trends Biochem. Sci. 32*, 101−110.
11. Chen, D., Walsby, C., Hoffman, B. M., and Frey, P. A. (2003) Coordination and mechanism of reversible cleavage of *S*-adenosylmethionine by the [4Fe-4S] center in lysine 2,3-aminomutase, *J. Am. Chem. Soc. 125*, 11788−11789.
12. Walsby, C. J., Hong, W., Broderick, W. E., Cheek, J., Ortillo, D., Broderick, J. B., and Hoffman, B. M. (2002) Electron-nuclear double resonance spectroscopic evidence that *S*-adenosylmethionine binds in contact with the catalytically active [4Fe-4S]+ cluster of pyruvate formate-lyase activating enzyme, *J. Am. Chem. Soc. 124*, 3143−3151.
13. Walsby, C. J., Ortillo, D., Broderick, W. E., Broderick, J. B., and Hoffman, B. M. (2002) An anchoring role for FeS clusters: Chelation of the amino acid moiety of *S*-adenosylmethionine to the unique iron site of the [4Fe-4S] cluster of pyruvate formate-lyase activating enzyme, *J. Am. Chem. Soc. 124*, 11270−11271.
14. Colichman, E. L., and Love, D. L. (1953) Polarography of sulfonium salts, *J. Org. Chem. 18*, 40−46.
15. Grimshaw, J. (1981) Electrochemistry of the sulphonium group, in *The Chemistry of the Sulphonium Group* (Stirling, C. J. M., and Patai, S., Eds.) Chapter 7, pp 141−155, Wiley & Sons Ltd., Chichester.
16. Saeva, F. D., and Morgan, B. P. (1984) Mechanism of one-electron electrochemical reductive cleavage reactions of sulfonium salts, *J. Am. Chem. Soc. 106*, 4121−4125.

17. Hinckley, G. T., and Frey, P. A. (2006) Cofactor-dependence in reduction potentials for $[4Fe\text{-}4S]^{2+/1+}$ in lysine 2,3-aminomutase, *Biochemistry 45*, 3219−3225.
18. Salmon, R. T., and Hawkridge, F. M. (1980) The electrochemical properties of three dypyridinium salts as mediators, *J. Electroanal. Chem. 112*, 253−364.
19. Magnusson, O. Th., Reed, G. H., and Frey, P. A. (2001) Characterization of an allylic analogue of the 5′-deoxyadenosyl radical: An intermediate in the reaction of lysine 2,3-aminomutase, *Biochemistry 40*, 7773−7782.
20. Markham, G. D., Hafner, E. W., Tabor, C. W., and Tabor, H. (1980) *S*-Adenosylmethionine synthetase from *Escherichia coli*, *J. Biol. Chem. 255*, 9082−9092.
21. Lees, N. S., Chen, D., Walsby, C. J., Behshad, E., Frey, P. A., and Hoffman, B. M. (2006) How an enzyme tames reactive intermediates: positioning of the active-site components of lysine 2,3-aminomutase during enzymatic turnover as determined by ENDOR spectroscopy, *J. Am. Chem. Soc. 128*, 10145−10154.
22. Spotswood, T. M., and Tanzer, C. I. (1967) N.M.R. Spectra and Stereochemistry of the Bipyridyls, *Aust. J. Chem. 20*, 1213−1225.
23. Ruzicka, F. J., Lieder, K. W., and Frey, P. A. (2000) Lysine 2,3-aminomutase from *Clostridium subterminale* SB4: Mass spectral chacterization of cyanogen bromide-treated peptides and cloning, *J. Bacteriol. 182*, 469−476.
24. Petrovich, R. M., Ruzicka, F. J., Reed, G. H., and Frey, P. A. (1991) Metal cofactors of lysine 2,3-aminomutase, *J. Biol. Chem. 266*, 7656−7660.
25. Beinert, H. (1983) Semi-micro methods for analysis of labile sulfide and of labile sulfide plus sulfane sulfur in unusually stable iron-sulfur proteins, *Anal. Biochem. 131*, 373−378.
26. Kennedy, M. C., Kent, T. A., Emptage, M., Merkle, H., Beinert, H., and Munck, E. (1984) Evidence for the formation of a linear [3Fe-4S] cluster in partially unfolded aconitase, *J. Biol. Chem. 259*, 14463−14471.
27. Chen, D., Frey, P. A., Lepore, B. W., Ringe, D., and Ruzicka, F. J. (2006) Identification of structural and catalytic classes of highly conserved amino acid residues in lysine 2,3-aminomutase, *Biochemistry 45*, 12647−12653.
28. Miller, J., Bandarian, V., Reed, G. H., and Frey, P. A. (2001) Inhibition of lysine 2,3-aminomutase by the alternative substrate 4-thialysine and Characterization of the 4-thialysyl radical intermediate, *Arch. Biochem. Biophys. 387*, 281−288.
29. Brazeau, B. J., Gort, S. J., Jessen, H. J., Andrew, A. J., and Liao, H. H. (2006) Enzymatic activation of lysine 2,3-aminomutase from *Porphyromonas gingivalis*, *Appl. Environ. Microbiol. 72*, 6402−6404.
30. Magnusson, O. Th., Reed, G. H., and Frey, P. A. (1999) Spectroscopic evidence for the participation of an allylic analogue of the 5′-deoxyadenosyl radical in the reaction of lysine 2,3-aminomutase, *J. Am. Chem. Soc. 121*, 9764−9765.
31. Finke, R. G., and Hay, B. P. (1984) Thermolysis of adenosylcobalamin: a product, kinetic, and cobalt-carbon (C5′) bond dissociation energy study, *Inorg. Chem. 23*, 3041−3043.
32. Magnusson, O. Th., and Frey, P. A. (2000) Synthesis and characterization of 3′,4′-anhydroadenosylcobalamin: A coenzyme B_{12} analogue with unusual properties, *J. Am. Chem. Soc. 122*, 8807−8813.
33. Lepore, B. W., Ruzicka, F. J., Frey, P. A., and Ringe, D. (2005) The x-ray crystal structure of lysine-2,3-aminomutase from Clostridium subterminale, *Proc. Natl. Acad. Sci. U.S.A. 102*, 13819−13824.
34. Wu, W., Lieder, K. W., Reed, G. H., and Frey, P. A. (1995) Observation of a second substrate radical intermediate in the reaction of lysine 2,3-aminomutase: A radical centered on the *β*-carbon of the alternative substrate, 4-thia-L-lysine. *Biochemistry 34*, 10532−10537.
35. Dayley, C. J. A., and Holm, R. H. (2001) Reactivity of $[Fe_4S_4(SR)_4]^{2-/3-}$ clusters with sulfonium cations: Analogue reaction systems for the inititial step in biotin synthase catalysis, *Inorg. Chem. 40*, 2785−2793.
36. Ugulava, N. B., Gibney, B. R., and Jarrett, J. T. (2001) Biotin synthase contains two distinct iron sulfur binding sites: chemical and spectroelectrochemical analysis of iron-sulfur interconversions, *Biochemistry 40*, 843−851.
37. Pierrel, F., Hernandez, H. L., Johnson, M. K., Fontecave, M., and Atta, M. (2003) MiaB protein from *Thermotoga maritima*. Characterization of an extremely thermophilic tRNA-methylthiotransferase, *J. Biol. Chem. 278*, 29515−29524.
38. Cosper, N. J., Booker, S. J., Ruzicka, F., Frey, P. A., and Scott, R. A. (2000) Direct FeS cluster involvement in generation of a radical in lysine 2,3-aminomutase, *Biochemistry 39*, 15668−15673.
39. Layer, G., Moser, J., Heinz, D. W., Jahn, D., and Schubert, W. D. (2003) Crystal structure of coproporphyrinogen III oxidase reveals cofactor geometry of Radical SAM enzymes, *EMBO J. 22*, 6214−6224.
40. Berkovitch, F., Nicolet, Y., Wan, J. T., Jarrett, J. T., and Drennan, C. L. (2004) Crystal structure of biotin synthase, an *S*-adenosylmethionine-dependent radical enzyme, *Science 303*, 767−769.
41. Hänzelmann, P., and Schindelin, H. (2004) Crystal structure of the *S*-adenosylmethionine dependent enzyme MoaA and its implications for molybdenum cofactor deficiency in humans, *Proc. Natl. Acad. Sci. U.S.A. 101*, 12870−12875.

BI701745H